www.amlett.org, www.amlett.com, DOI: 10.5185/amlett.2012.icnano.230
"ICNANO 2011" Special Issue Published online by the VBRI press in 2012

Effect of barrier height on linear and nonlinear photoabsorption and refractive index change in Si quantum dots

Anchala*, S. P. Purohit, and K. C. Mathur

Department of Physics and Materials Science and Engineering,
Jaypee Institute of Information Technology, A-10, Sector 62, Noida, U.P. 201307, India

*Corresponding author. Tel: (+91) 120 2594279; E-mail: anchalajiit@gmail.com

ABSTRACT

The effect of barrier height on the photoabsorption process and refractive index changes are studied for the intraband transitions in spherical single electron Si quantum dots embedded in dielectric matrix. We use the effective mass approximation and consider (i) the finite, and (ii) infinite barrier height at the interface of the dot and matrix material. The results obtained for the dipole allowed S-P transition show that the increase in barrier height leads to blue shift in peak positions of absorption coefficient and refractive index change. We also investigate the effect of intensity and dot radius on the above parameters.

Keywords: Quantum dot; barrier height; nonlinear; photoabsorption.

Anchala received M.Sc. degree in Physics in 2003 M. J. P. Rohilkhand University Bareilly. She is currently pursuing Ph.D. degree. Her research interests include study of semiconductor nanostructures.

S. P. Purohit did Ph. D. in physics from the Physics Department, University of Roorkee in 1992. He is working as Associate Professor at JIIT, Noida.

K. C. Mathur received Ph. D. degree in 1971. He joined University of Roorkee, India as faculty in 1963 and worked there for 37 years. He has over 100 publications in international journals. He joined JIIT, Noida, in 2001 as Professor and Head of Physics Department.

Introduction

Quantum dots behave like artificial atoms and their electronic and optical properties are significantly different as compared to bulk **[1].** In the interaction of radiation with matter at low radiation intensity the induced polarization depends linearly on the electric field and linear response is obtained in absorption of radiation. However, when the intensity is increased nonlinear terms in induced polarization become important which lead to nonlinear optical properties. The linear and nonlinear optical absorption in dots is significantly different from that of bulk because the dipole matrix elements of the optical transitions in the sub bands of the dot have large values **[2].** The linear absorption depends on the square of the dipole matrix and the nonlinear response on the 4^{th} power of the transition matrix. Hence the linear and nonlinear properties are enhanced in nanostructures. This has also been found experimentally **[3-6].**

The intraband transitions in quantum dots are important being mostly in the infrared region. The nonlinear optical properties of semiconductor quantum dots have attracted considerable interest due to their relevance to several technological applications in optoelectronics and nano photonics e.g. in far-infrared laser amplifiers, photo detectors **[7],** high speed electro – optical modulators **[8]** and optical switches **[3].** The optical properties of a quantum dot can be tailored by changing the shape and size of the dot, the confining potential at the interface of the dot and its surrounding matrix, and the energy and intensity of incident radiation.

The silicon quantum dot embedded in SiO_2 dielectric matrix is of particular interest due to significant technological applications such as in single electron memory devices, complementary metal oxide semiconductor (CMOS), and silicon photonics **[4].** Several theoretical and experimental studies **[2-6, 9–18]** are reported in the literature for linear and nonlinear optical properties of quantum dots. In most of experimental studies photo induced interband transitions are reported **[3–6].** Studies on the nonlinear optical properties of Si quantum dots are not yet fully explored; however, such studies would be useful for several photonic devices based on the nonlinearity. Since the crystalline Si is centrosymmetric, the second order susceptibility vanishes and the third order is the lowest nonlinearity **[19].**

Yildirim and Bulutay **[9]** used an atomistic pseudopotential approach to study nonlinear optical properties of Si and Ge nanocrystals embedded in SiO_2 matrix. Chaojin et al. **[12]** studied the nonlinear optical absorption coefficient and refractive index changes in a GaAs /AlGaAs two- dimensional system. Recently, Yilmaz et al. **[13]** reported the third – order nonlinear absorption spectra of an impurity in a spherical quantum dot of GaAs with different confining potential.

In this paper we study the effect of change of barrier height on the linear and nonlinear optical properties of the Si quantum dot for different incident optical intensities and dot radii. We use the effective mass approximation and consider finite and infinite barrier height at the interface of the dot and the matrix material. Results are obtained for linear and nonlinear absorption coefficients, the refractive index change with the variation of dot size, incident photon energy and intensities. We include the effect of the local field and the dot size dependence of the dielectric constant **[20].** The effect of the self-energy **[21]** associated with the charging of the dot is also considered.

Wave functions and energy levels

The wave functions and energy levels of the bound states are calculated by solving the Schrödinger wave equation for an electron in spherical quantum dot of barrier height $V_{eff}(r)$ as,

$$\left[-\frac{\hbar^2}{2}\vec{\nabla}(m^{-1}\vec{\nabla})+V_{eff}(r)\right]\psi(\vec{r})=E\psi(\vec{r}) \qquad (1)$$

where m is the effective mass tensor. We replace the effective mass tensor m by a scalar effective mass which is taken as a harmonic mean of the transverse and longitudinal masses as [**22**],

$$\frac{1}{m^*_{Si}}=\frac{1}{3}\left[\frac{1}{m_L}+\frac{2}{m_T}\right]$$

where, m_L and m_T is the longidudnal and transverse mass, with $m_L=0.92m_e$ and $m_T=0.19m_e$. m_e is the mass of free electron.

The eigen functions and eigen values of the confined states are obtained by solving the Schrödinger equation (1) for infinite and the finite barrier height.

Infinite barrier

For the infinite barrier height at the interface of the dot and matrix, we take

$$V_{eff}(r)=0 \text{ for } r<R \text{ and } V_{eff}(r)=\infty \text{ for } r\geq R \qquad (2)$$

The wave functions and the energy levels of the confined states are given by,

$$\psi(\vec{r})=R_{n\ell}(r)Y_{\ell m}(\hat{r}) \qquad (3)$$

where the radial part

$$R_{n\ell}=Aj_\ell\left(\frac{\xi_{n\ell}r}{R}\right) \qquad (4)$$

and $$E_{n\ell}=\frac{\hbar^2}{2m^*_{Si}R^2}\xi^2_{n\ell} \qquad (5)$$

where, A is the normalization constant and $\xi_{n\ell}$ is the nth zero of the spherical Bessel function $j_\ell(z)$

Finite Barrier

Considering the case of finite barrier height at the interface of the dot and matrix material we take,

$$V_{eff}(r)=0 \text{ for } r<R$$
$$\text{and } V_{eff}(r)=V_0+\Sigma \text{ for } r\geq R \qquad (6)$$

where V_0 is the confinement potential at the interface of Si dot and surrounding matrix. Σ is the self energy associated with the charging of the quantum dot with an electron. Using equation (6) the solution of the Schrödinger wave equation (1) can be written as, $\psi(\vec{r})=R_{n\ell}(r)Y_{\ell m}(\hat{r})$ with the radial part of the wave function $R_{n\ell}$ given by,

$$R_{n\ell}(r)=Aj_\ell(\alpha r) \text{ for } r<R$$
$$\text{and } R_{n\ell}(r)=Bk_\ell(\beta r) \text{ for } r\geq R \qquad (7)$$

where A and B are the normalization constants and j_ℓ and k_ℓ are the spherical Bessel and the modified spherical

Bessel functions respectively. α and β are obtained by using appropriate boundary conditions **[15]** at $r = R$.

We consider the surrounding matrix of SiO_2 with different confinement potential V_0 of heights 0.5 eV, 3.1 eV and infinite. The effective electron mass in the Si dot and SiO_2 matrix is taken as $m^*_{si} = 0.27m_e$ and $m^*_{SiO_2} = 0.5m_e$ respectively. The dielectric constants are taken as $\varepsilon_{in} = 11.7$ and $\varepsilon_{out} = 3.8$. Where ε_{in} and ε_{out} are dielectric constants for the dot material and the matrix material respectively. The size dependence of the dielectric constant ε_{in} of the dot of radius R is taken as **[20],**

$$\varepsilon_{in}(R) = 1 + (\varepsilon^b_{in} - 1)\left(1 + \left(\frac{\gamma}{R}\right)^{\ell}\right)^{-1} \quad (8)$$

where the dielectric constant of the bulk $\varepsilon^b_{in} = 11.4$, $\gamma = 0.92nm$, and $\ell = 1.18$. The inclusion of the self energy Σ slightly increases the barrier height.

Linear and nonlinear optical properties

The linear photoabsorption coefficient $\alpha^{(1)}(\omega)$ and nonlinear $\alpha^{(3)}(\omega)$ photoabsorption coefficient between two intersubband levels is given by [10, 15],

$$\alpha^{(1)}(\omega) = \sum_{if} \frac{\sigma_v \pi \omega e^2}{c n_r \varepsilon_0} |M_{fi}|^2 \delta(E_f - E_i - \hbar\omega) \quad (9)$$

$$\alpha^{(3)}(\omega, I) = -\sum_{if} \frac{2I\sigma_v \pi^2 \omega e^4}{c^2 n_r^2 \varepsilon_0^2 \hbar\Gamma} |M_{fi}|^4 \delta^2(E_f - E_i - \hbar\omega) \quad (10)$$

with the delta function defined as

$$\delta = \frac{\hbar\Gamma}{\pi[(E_f - E_i - \hbar\omega)^2 + (\hbar\Gamma)^2]}$$

σ_v is the carrier density in the quantum dot, ε_0 is the permittivity of free space. E_i and E_f are the energies of the initial and the final states of the dot and Γ is the linewidth, we take $\hbar\Gamma$=6meV. The dipole transition matrix is $M_{fi} = F\langle\psi_f|\vec{r}.\hat{\varepsilon}|\psi_i\rangle$. F is the local field factor, which relates the electric field inside the dot E_{in} to the electric field outside the dot E_{out} by $E_{in} = FE_{out}$ It is given by [**21**], $F = 3\varepsilon_{out}/(\varepsilon_{in} + 2\varepsilon_{out})$. n_r is the refractive index of the dot material, c is the velocity of light. $\hat{\varepsilon}$ is the unit polarization vector of the incident linearly polarized photon, I is the incident optical intensity, and $\hbar\omega$ is the incident photon energy.

The total photoabsorption coefficient is,

$$\alpha(\omega, I) = \alpha^{(1)}(\omega) + \alpha^{(3)}(\omega, I) \quad (11)$$

The linear and the nonlinear refractive index is given by [**10**],

$$\frac{\Delta n^{(1)}(\omega)}{n_r} = \frac{\sigma_v e^2}{2n_r^2 \varepsilon_0} |M_{fi}|^2 \left(\frac{E_f - E_i - \hbar\omega}{[(E_f - E_i - \hbar\omega)^2 + (\hbar\Gamma)^2]}\right) \quad (12)$$

$$\frac{\Delta n^{(3)}(\omega, I)}{n_r} = -\frac{I\mu c}{n_r^3 \varepsilon_0} \sigma_v e^4 |M_{fi}|^4 \left(\frac{E_f - E_i - \hbar\omega}{[(E_f - E_i - \hbar\omega)^2 + (\hbar\Gamma)^2]^2}\right) \quad (13)$$

and the total refractive index change is

$$\frac{\Delta n\ (\omega, I)}{n_r} = \frac{\Delta n^{(1)}(\omega)}{n_r} + \frac{\Delta n^{(3)}(\omega, I)}{n_r} \quad (14)$$

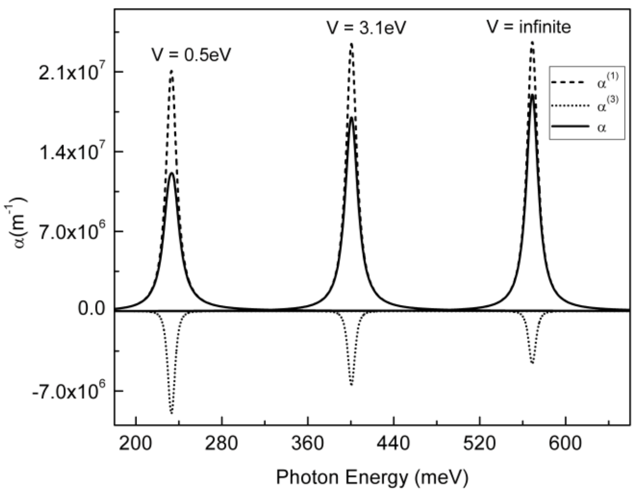

Fig. 1. The variation of linear, nonlinear, and total photoabsorption coefficient as a function of the incident photon energy with I=20 MW/cm^2 and dot radius R=16Å.

The third order nonlinear ($\chi^{(3)}$) optical susceptibility is given by,

$$\varepsilon_0 \chi^{(3)}(\omega) = -\frac{\sigma_v e^4 4|M_{fi}|^4 |E(\omega)|^2}{(E_f - E_i - \hbar\omega - i\hbar\Gamma)[(E_f - E_i - \hbar\omega)^2 + (\hbar\Gamma)^2]} \quad (15)$$

Results and discussion

Fig. 1 shows the effect of the increase of the barrier height on the linear $\alpha^{(1)}(\omega)$, the third order nonlinear $\alpha^{(3)}(\omega, I)$ and the total photoabsorption coefficient $\alpha(\omega, I)$ at fixed dot radius and fixed incident optical intensity. The absorption coefficients are plotted as a function of the incident photon energy for three barrier heights (0.5 eV, 3.1 eV and infinite) at dot radius R=16Å and intensity I=20 MW/cm^2. It is observed that the magnitude of the linear photoabsorption coefficient increases with increase in the barrier height. The increase of the linear photoabsorption coefficient with the barrier height is attributed to the increase in overlap of wave functions of the ground and excited states. The nonlinear photoabsorption coefficient which is negative decreases in magnitude with increase of barrier height. This is due to the decrease of the transition matrix with increase in the barrier height. The total photoabsorption coefficient, which is the sum of the linear and the third order nonlinear parts increases with the increase of barrier height. It is observed that the peak position of the total absorption coefficient $\alpha(\omega, I)$ is blue shifted with the increase in barrier height. The nature of the shift in the peak position can be explained by considering the variation of the transition energy with the dot size (which for a given size increases with increase in barrier height **[15]**).

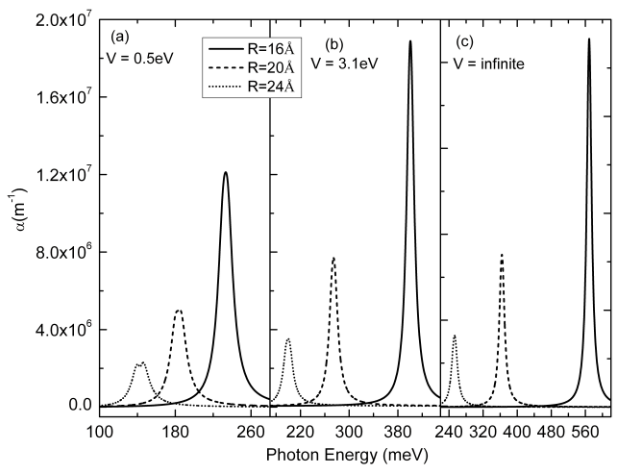

Fig. 2. The variation of the total photoabsorption coefficient as a function of photon energy at different values of the dot radii R at I=20 MW/cm^2

Fig. 2 shows the effect of the increase of barrier height on the total photoabsorption coefficient $\alpha(\omega, I)$ at different dot radii (R=16Å, 20Å, and 24 Å) at a fixed intensity of incident radiation I=20 MW/cm^2. It is observed that for all quantum dot radii the peak value of total photoabsorption coefficient increases with the increase of barrier height. At large dot size and smaller value of barrier height the bleaching effect is observed where a single peak splits into two peaks. The bleaching at large dot size occurs due to increase of the nonlinear photoabsorption coefficient (which is negative). This is because the nonlinear photoabsorption coefficient is proportional to fourth power of transition matrix, (which increases with the decrease in barrier height and increases with the increase of dot size). The peak value of the total photoabsorption coefficient increases with the decrease of the dot radius. This is because the optical absorption coefficient depends inversely on the volume of the quantum dot. The peak position of total photoabsorption coefficient shows red shift with the increase of the dot radius. This is because the transition energy decreases with the increase in the dot radius.

Fig. 3 shows the effect of increase of the barrier height on the total photoabsorption coefficient $\alpha(\omega, I)$ with the increase in intensity of incident radiation at fixed dot radius. For three barrier heights (0.5 eV, 3.1 eV and infinite) we take three different intensities (I=20, 30, and 40 MW/cm^2) and fixed dot radius R=16Å. It is observed that at sufficiently high intensity 30 MW/cm^2 bleaching is noticed at smaller value of barrier height. Also the total photoabsorption coefficient decreases with the increase in intensity of the incident radiation. This is due to the increase of negative contribution of nonlinear photoabsorption coefficient at higher intensity.

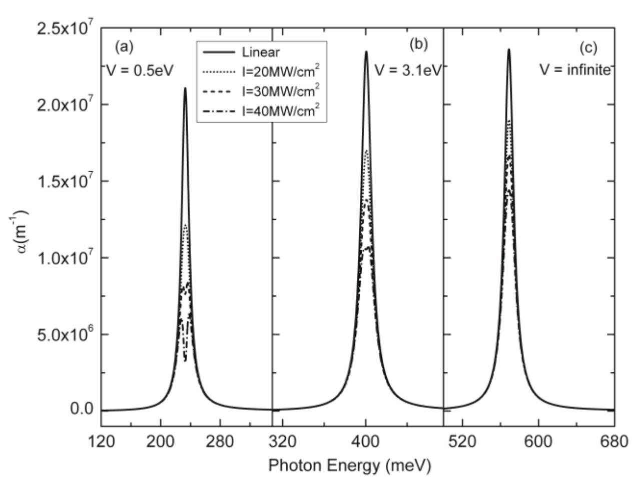

Fig. 3.The variation of the total photoabsorption coefficient as a function of photon energy at different values of intensities and the dot radius R=16 Å.

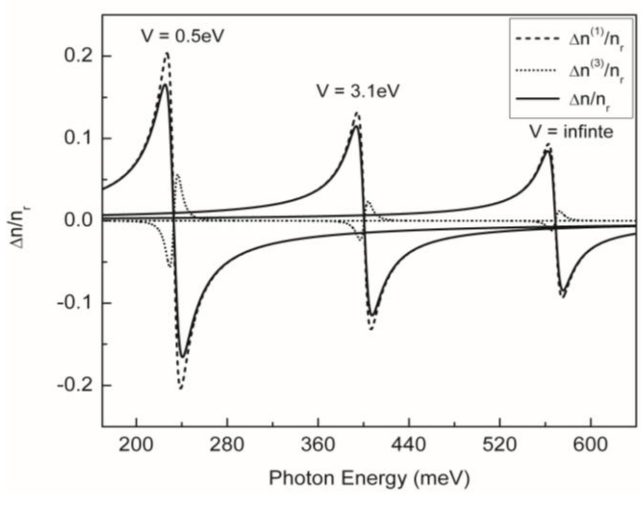

Fig. 4. The variation of linear, nonlinear, and total change in refractive index as a function of the incident photon energy with I=20 MW/cm^2 and R=16Å.

Fig. 4 shows the effect of the increase of barrier height on the refractive index change of the Si quantum dot at a fixed dot radius and intensity of incident radiation. Results are plotted for the variation of the linear $\frac{\Delta n^{(1)}(\omega)}{n_r}$, third order nonlinear $\frac{\Delta n^{(3)}(\omega)}{n_r}$, and total refractive index change $\frac{\Delta n(\omega)}{n_r}$ as a function of photon energy at the dot radius R=16Å and at incident intensity I=20 MW/cm^2. It is noticed that the maximum value of linear refractive index change decreases with the increase in the barrier height. This is due to decrease in the value of the transition matrix at larger value of barrier height. The resonance position which is the position of zero crossing of the total refractive index change is blue shifted with increase of the barrier height. This is due to the increase in energy difference between the energy levels with the increase in barrier height. The total refractive index change (which is the sum of linear and nonlinear parts) reduces due to the negative contribution of the nonlinear term.

Fig. 5 shows the effect of the increase of barrier height on the total refractive index change for different dot radius (R=16 Å, 20Å, and 24 Å) at fixed intensity I=20 MW/cm^2. It is observed that at each dot radii the magnitude of total refractive index change decreases with the increase in barrier height. Also the resonance position of total refractive index change shifts towards lower energy with the increase in dot radius. This is because the threshold energy decreases with the increase in dot radius.

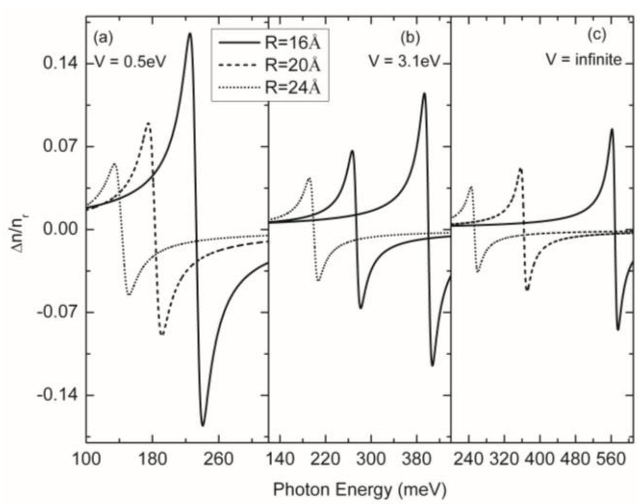

Fig. 5. The variation of total change in refractive index as a function of the incident photon energy at different values of the dot radii R at I=20 MW/cm^2.

Fig. 6 shows the effect of the increase of barrier height on the total refractive index change at intensities I=20 MW/cm^2, 30 MW/cm^2, and 40 MW/cm^2 at a fixed dot radius R=16Å. It is observed that the magnitude of total refractive index change decreases with the increase in barrier height at all three intensities. For all three barrier heights the total refractive index change decreases with the increase in the intensity of incident radiation. This is due to the increase of the negative contribution of the nonlinear term which increases with the increase in intensity.

Fig 7 shows the effect of the increase of barrier height on the third order nonlinear susceptibility $\left|\chi^{(3)}(\omega)\right|$ at a fixed dot radius R=16Å and at a fixed intensity of incident radiation I=20 MW/cm^2. It is observed that the absolute value of third order nonlinear optical susceptibility decreases with the increase of barrier height. This is due to the decrease of transition matrix with the increase in barrier height.

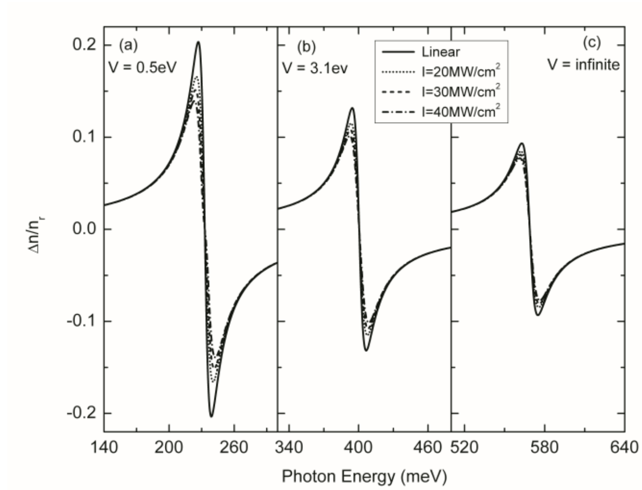

Fig. 6. The variation of total change in refractive index as a function of the incident photon energy at different values of intensities at dot radius R=16 Å.

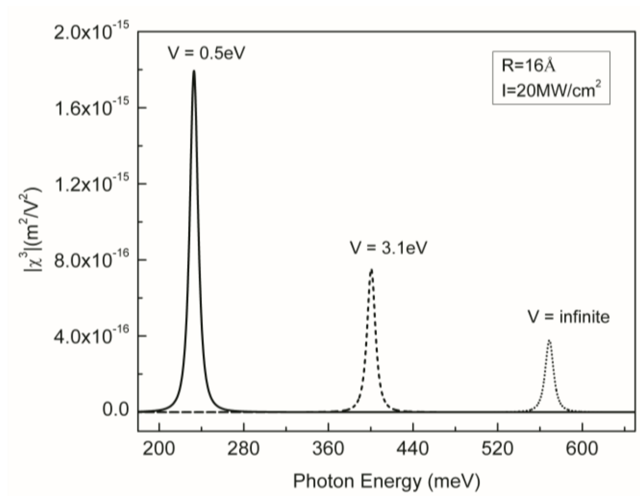

Fig. 7. The variation of third order optical susceptibility as a function of the incident photon energy with I=20 MW/cm^2 at R=16 Å.

Conclusion

We have investigated the effect of barrier height on the linear, nonlinear, and total photoabsorption coefficient and the refractive index change of a single electron charged spherical Si quantum dot embedded in the amorphous SiO_2 matrix. From this study we conclude that the peak position of photoabsorption coefficient is blue shifted with the increase of the barrier height and red shifted with the increase in dot radius. The peak value of the total photoabsorption coefficient increases with the increase of the barrier height. However, the total refractive index change, and absolute value of third order nonlinear optical susceptibility decrease with the increase of the barrier height. Also the total photoabsorption coefficient and the refractive index change decrease in magnitude with the increase of optical intensity. The present study about the effect of the barrier height on the nonlinear optical properties would be useful in optoelectronic devices based on Si quantum dots.

Acknowledgment

We thank the Jaypee Institute of Information Technology, Noida for providing facilities and support to carry out this work.

References

1. Yoffe, A. D. *Adv. Phys.* 2001, 50, 1.
   DOI: 10.1080/00018730010006608
2. Rezaei, G.; Mousazadeh, Z.; Vaseghi, B. *Physica E* 2010, 42, 1477.
   DOI:10.1016/j.physe.2009.11.122
3. Henari, F. Z.; Morgenstern, K.; Blau, W. J.; Karavanskii, V. A.; Dneprovskii, V. S. *Appl. Phys. Lett.* 1995, 67, 323.
   DOI: 10.1063/1.115432
4. Bettotti, P.; Cazzanelli, M.; Negro, L. D.; Danese, B.; Daness, Z.; Gaburro, Z.; Oton, C. J. Prakash, G. V.; Pavesi, L. *J. Phys. Condens. Matter*, 2002, 14, 8253.
   DOI: 10.1088/0953-8984/14/35/305
5. Vijayalakshmi, S.; Lan, A.; Iqbal, Z.; Grebel, H. *J. Appl. Phys.* 2002, 92, 2490.
   DOI: 10.1063/1.1498881
6. Imakita, K.; Ito, M.; Fujii, M.; Hayashi, S. *J. Appl. Phys.* 2009, 105, 093531.
   DOI: 10.1063/1.3125446
7. Miller, D. A. B. *Int. J. High Speed Electron. Syst.* 1990, 1, 19.
   DOI: 10.1142/S0129156490000034
8. Wood, T.H. J. *Lightwave Technol.*1988, 6, 743.
   DOI: 10.1109/50.4063
9. Yildirm, H.; Bulutay, C. *Phys. Rev. B.* 2008, 78, 115307.
   DOI: 10.1103/PhysRevB.78.115307
10. Sahin, M. *J. Appl. Phys.* 2009, 106, 063710.
    DOI: 10.1063/1.3225100
11. Ozmen, A.; Yakar, Y.; Cakir, B.; Atav, U. *Opt. Commun.* 2009, 282, 3999.
    DOI: 10.1016/j.optcom.2009.06.043
12. Zhang, C.; Wang, Z.; Gu, M.; Liu, Y.; Guo, K. *Physica B.* 2010, 405, 4366.
    DOI: 10.1016/j.physb.2010.07.044
13. Yilmaz, S.; Sahin, M. *Phys. Status Solidi B.* 2010, 247, 371.
    DOI: 10.1002/pssb.200945491
14. Ito, M.; Imakita, K.; Fujii, M.; Hayashi, S. *J. Appl. Phys.* 2010, 108, 063512.
    DOI: 10.1063/1.3480821
15. Anchala; Purohit, S. P.; Mathur, K. C. *Appl. Phys. Lett.* 2011, 98, 043106.
    DOI: 10.1063/1.3548861
16. Kostic, R.; Stojanovic, D. *J. of Nanophotionics.* 2011, 5, 051810.
    DOI: 10.1117/1.3599444
17. Kirak, M.; Yilmaz, S.; Sahin, M.; Gencaslan, M. *J. Appl. Phys.* 2011, 109, 094309.
    DOI: 10.1063/1.3582137
18. Yilmaz, S.; Safak, H.; Sahingoz, R.; Erol, M., *Cent. Eur. J. Phys.* 2010, 8, 438.
    DOI: 10.2478/s11534-009-0115-8
19. Robert, W. B., *Nonlinear Optics* 2003, (Academic, San Diego).
20. Lannoo, M.; Delerue, C.; Allan, G. *Phys. Rev. Lett.* 1995,74, 3415
    DOI: 10.1103/PhysRevLett.74.3415
21. C. Delerue, M. Lannoo, *Nanostructures: Theory and Modeling* (Springer, Berlin, 2004).
22. See, J.; Dollfus, P.; Galdin, S. *Phys. Rev. B.* 2002, 66, 193307.
    DOI: 10.1103/PhysRevB.66.193307